Title
Flexural behavior of preloaded reinforced concrete beams strengthened by prestressed CFRP laminates

Journal
COMPOSITE STRUCTURES, 157

ISSN
0263-8223

Authors
Gao, P
Gu, X
Mosallam, AS

Publication Date
2016-12-01

DOI
10.1016/j.compstruct.2016.08.013

Peer reviewed

Push-out tests for perfobond strip connectors with UHPC grout in the joints of steel-concrete hybrid bridge girders

Article *in* Engineering Structures · March 2017

DOI: 10.1016/j.engstruct.2017.01.008

CITATIONS
0

READS
42

3 authors:

He Shao-hua
University of California, Irvine
6 PUBLICATIONS **4** CITATIONS
SEE PROFILE

Zhi Fang
Hunan University
69 PUBLICATIONS **230** CITATIONS
SEE PROFILE

Ayman S. Mosallam
University of California, Irvine
134 PUBLICATIONS **1,121** CITATIONS
SEE PROFILE

Engineering Structures 135 (2017) 177–190

Contents lists available at ScienceDirect

Engineering Structures

journal homepage: www.elsevier.com/locate/engstruct

Push-out tests for perfobond strip connectors with UHPC grout in the joints of steel-concrete hybrid bridge girders

Shaohua He [a], Zhi Fang [a,*], Ayman S. Mosallam [b]

[a] College of Civil Engineering, Hunan University, Changsha, Hunan 410082, China
[b] Department of Civil and Environmental Engineering, University of California, Irvine, CA 92697, USA

ARTICLE INFO

Article history:
Received 7 March 2016
Revised 2 January 2017
Accepted 4 January 2017

Keywords:
Perfobond strip connector
Steel-concrete joints
Ultra-high performance concrete (UHPC)
Ultimate strength
Push-out tests

ABSTRACT

This paper aims at examining the structural behavior of perfobond strip (*PBL*) connectors for steel-concrete joint of hybrid girders with ultra-high performance concrete (*UHPC*) as grout for such connectors. Twenty-four push-out specimens fabricated according to the design used for the connectors in the steel-concrete joint in a hybrid cable-stayed bridge have been investigated. Effects of several parameters such as (i) the interface bond between perforated plate and concrete, (ii) dowels inside the holes in the plate, and (iii) volume of steel fibers in the UHPC on the behavior of PBL were discussed in depth. Experimental results indicated that the use of a 2% volume fraction of steel fibers in the UHPC, increased the average bond strength at the plate/concrete interface and the shear resistant-capacity of concrete dowel by 82% and 50%, respectively, as compared to UHPC specimens without the fibers. The concrete dowel played an important role in developing the desired loading resistant-capacity of the PBL, and about 34–41% of the overall resistance of a standard PBL embedded in UHPC were supplied by the concrete dowel surrounding transverse rebar. The source of the achieved ductility of PBL was mainly determined by the action of transverse rebars, and the ductility in the specimens having transverse rebars was about eleven times the ductility of similar specimens without the rebars. Furthermore, the experimental ultimate strength values of PBL were compared with available equations in literatures published recently, and an analytical model for PBL/UHPC was developed and appropriate parameters were derived from present data and used to provide reliable prediction of ultimate resistant-capacity of PBL in the hybrid girders' steel-concrete joints.

1. Introduction

Due to the excellent economical, constructional, and mechanical advantages, steel/concrete composite structures have been widely used in civil infrastructural applications. The most common composite structural system is comprised of a steel girder topped with a reinforced concrete (*RC*) slab for both buildings and bridge applications. Another form of composite structure that attracted engineers' attention nowadays is the steel-concrete hybrid girders. These hybrid girders have remarkable advantages in terms of structural behavior. Compared with the conventional superimposed beams, a hybrid girder consists of both steel and RC girders that are connected in series via a steel-concrete joint. In this case, shear connectors are required for transmitting forces between steel and RC girders. One of the most popular connectors is the headed steel studs due to their rapid application and their efficient structural behavior. The performance of steel studs in composite structure has been extensively investigated in recent years [1–3]. However, the insufficient fatigue property and harsh requirements on installation equipment of steel stud connectors has limited their further application [4].

In 1980s, Leonhardt [5] proposed the Perfobond strip (PBL) connector that is composed of perforated steel plates and reinforced concrete dowels as shown in Fig. 1. The ease of construction coupled with their superior mechanical performance made PBL connectors to be widely used. These connectors can be used in lieu of traditional steel studs for shear transfer in steel-concrete composite structures.

The main differences between the PBLs in superimposed beams and those in steel-concrete joints of hybrid girders are in their failure modes and mechanical properties. In superimposed beams, PBLs are embedded in a relatively thin RC floor slabs or bridge deck that typically the failure usually occurs due to cracking of slabs. In comparison, PBLs in steel-concrete joint of hybrid girders are plugged deeply in concrete blocks and their failure modes

* Corresponding author.
E-mail address: fangzhi@hnu.edu.cn (Z. Fang).

http://dx.doi.org/10.1016/j.engstruct.2017.01.008
0141-0296/

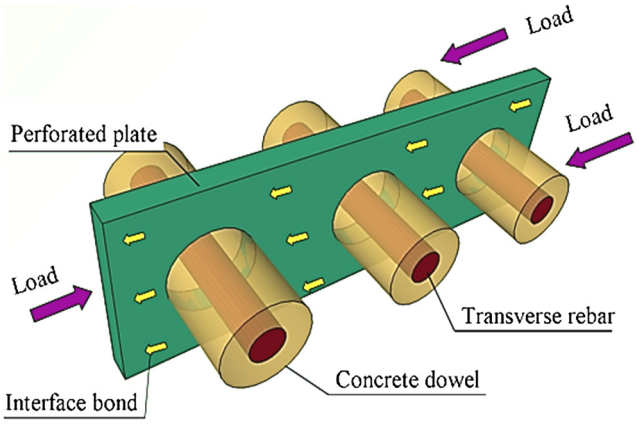

Fig. 1. Load transfer principle of perfobond strip connectors.

generally governed by fracture of the dowels by the holes. Meanwhile, PBLs in hybrid girders have much stronger interfacial restraints and the interfacial bond at the contact surface between perforated plate and concrete is more significant as compared with those in the superimposed beams [6]. As sufficient quantity of PBLs are used to transfer the major shear forces between steel components and concrete in hybrid girders, the effect of local concrete at the end of the perforated plate is small and can be negligible [7–9].

Mechanical behavior of PBL in superimposed beams with the use of conventional concrete has been experimentally and numerically assessed by several researchers. For example, Leonhardt et al. [5] and Hans-Peter [10] performed push-out tests of PBL to determine the performance of the connector. The experimental results indicated that PBL resistance was primarily influenced by concrete strength and hole diameter in perforated plate. Oguejiofor and Hosain [11,12] reported the results of an experimental study performed on sixty-one push-out specimens and conducted comprehensive numerical simulations for predicting the capacity of PBL embedded in concrete slabs. Based on their study, it was found that the interlock effect of adjacent holes in perforated plate could be eliminated by spacing larger than 2.25 times the hole diameter. Ahn et al. [13] performed fourteen push-out tests involving the arrangement of perforated plate, type and strength of concrete, and presence of transverse rebar. In this study, equations for determining the PBL capacity for structural design of the connectors in superimposed beams were presented. Studnicka et al. [14] performed sixty-one push-out tests to evaluate the capacity and behavior of PBL embedded in both normal and lightweight concrete slabs. Based on this study, it was shown that the shear capacity of PBL was significantly affected by both the compressive strength and the modulus of elasticity of concrete. Similar conclusions were reported by Valente et al. [15,16]. Medberry et al. [17] performed a total of twenty-eight push-out tests to examine the effects of chemical bond between the steel girder flange and the concrete slab. The contribution of chemical bond to shear capacity of PBL was considered in their proposed equation for evaluating the shear resistance. Al-Darzi et al. [18] proposed a numerical model using the finite element method to simulate the push-out tests. The effectiveness of the model was verified by the experimental results. A comprehensive discussion on the behavior of PBL embedded in concrete slabs was presented by Candido-Martins et al. [19]. Further experimental and numerical studies varying with the concrete strength, number of holes, and the concrete slab thickness were performed by Vianna et al. [20], and an equation to predict the shear capacity of PBL with different concrete strength was proposed.

In the past few years, research studies on the behavior of PBL with conventional concrete in steel-concrete joint of hybrid girders were performed. Wang et al. [6] performed twenty-four push-out tests to study the mechanical behavior of PBL in hybrid girders. It was shown that the interface bond between perforated plate and surrounding concrete substantially increased due to the strong restraints on the plate resulted from the reinforcements in concrete blocks. He et al. [7] conducted six push-out tests and a large-scale model test to examine the shear strength and reliability of PBL in steel-concrete joint of hybrid girders. The results revealed that the shear resistance of a PBL in a twin configuration was about 80% of that of a single independent PBL and the connectors effectively transferred the forces in steel-concrete joint. Zheng et al. [21] presented results from twenty-one push-out tests of PBL embedded in conventional concrete involving both hole diameter and shape. It was concluded that the shear stiffness of the connector was improved with the increase of hole diameter. An analytical model to determine the shear capacity of PBL regardless of the hole geometry was suggested by the authors. He et al. [22] performed twelve push-out tests to study the load transferring mechanism of PBL embedded in conventional concrete in steel-concrete joint. Results of the study indicated that the mechanical properties of PBL in hybrid girders were improved due to the bond at plate/concrete interface, and corresponding equation for determining the shear capacity of PBL with conventional concrete in hybrid girders was proposed.

In the recent years, studies on the behavior of PBL in ultra-high performance concrete (UHPC) have also been found in literature. For example, Hegger et al. [23,24] investigated the behavior of puzzle strip connectors using UHPC slabs with compressive strength of 180 MPa. It was found that the continuous type of shear connectors like the puzzle strip were appropriate for the UHPC by carrying high shear loads with appropriate ductility. Kang et al. [25] performed tests on fourteen push-out specimens of PBL with UHPC slabs. The results indicated that the shear capacity of PBL in superimposed beams was improved by increasing the strength of UHPC. Wirojjanapirom et al. [26] investigated the efficiency of using UHPC to improve the shear capacity of PBL by twelve pre-stressed short-beam tests. Results of the study showed an increase of PBL shear capacity due to the application of pre-stressing force.

Concrete-filled steel-concrete joint in hybrid girders should have sufficient strength and durability to ensure the shear capacity of connectors in the joint. However, with the extensive use of conventional concrete in steel-concrete joints, many problems arise. For example, the quality of poured concrete with coarse aggregate in the joint is difficult to be guaranteed due to the heavy reinforcements and the presence of pre-stressing tendons in the steel-concrete joint zone. In addition, the separation between steel plate and concrete is difficult to be avoided due to the shrinkage of conventional concrete at the joint zone. These two issues are harmful to the integrity of the connectors. The use of UHPC can be a way to solve these problems. UHPC has many remarkable advantages such as ultra-high strength, better ductility, and excellent durability owing to its homogenized microstructure and the incorporation of fibers. The less creep and shrinkage characteristics of UHPC may result in better bond between joint steel components and concrete, and the higher strength of UHPC and absence of coarse aggregates may also contribute to reducing the required number of PBLs in addition to the ease of placing the concrete at the joint zone.

Recently, UHPC has been successfully applied to the steel-concrete joint of Nujiang Bridge, which is a steel-concrete hybrid cable-stayed bridge with a span arrangement of 81 m + 175 m, located in Yunan, China. Although some studies were carried out on performance of PBL using UHPC in superimposed beams, however, few studies reported the behavior of PBL with UHPC in

steel-concrete joint in hybrid girders. Considering the high fracture energy and high strength of UHPC, the effects of interfacial bond and dowels by the hole may be different. Also, the existing equations for predicting the ultimate resistances of PBL were developed based on test results performed on conventional concrete with comparatively low strength, equations to predict shear resistance of PBL with UHPC in steel-concrete joint of hybrid girders is not available.

This study aims at evaluating the mechanical behavior of PBL in steel-concrete joint of hybrid girders with the use of UHPC as the grout in the joint through twenty-four push-out specimens. Test parameters included (i) bond state at perforated plate/concrete interface, (ii) presence of concrete dowel and transverse rebar in the hole, and (iii) the steel fiber volume in the UHPC. The availability of the existing equations for predicting the ultimate resistance of PBL using conventional concrete is discussed by the present test results, and an improved equation for the ultimate shear capacity of PBL in steel-concrete joint of hybrid girders with the use of both conventional concrete and UHPC is developed.

2. Description of experimental program

2.1. Push-out test specimens

In order to investigate the structural behavior of PBL in steel-concrete joint using UHPC grout, twelve groups of PBL connectors, 24 specimens in total, were fabricated and tested by means of the push-out test method developed by Su et al. [8]. As shown in Table 1, the test parameters adopted in these tests were (i) bonding state at the perforated plate/concrete interface, (ii) presence of concrete dowel and transverse rebar by the hole in plate, and (iii) volume of steel fibers in UHPC.

Specimen labels shown in Table 1 start with R or RF standing for Reactive Powder Concrete without steel fibers (*RPC*) or Reactive Powder Concrete with steel fibers (*RPCF*). The following letters b, r, and d represent the interface bond, the transverse rebar and the concrete dowel near the hole, respectively, and the number 1 or 0 after the b, r, or d indicates whether the corresponding part exists, with 1 for Yes and 0 for No. For example, "RF-b1r0d1" indicates a specimen fabricated using RPCF, and the specimen has bond at the plate/concrete interface and a concrete dowel near the hole but no transverse rebar passing through the hole.

The pure bond specimens, only with bond at the steel plate surface, were designed to study the bonding effects at the plate/concrete interface. The unbonded concrete dowel specimens, consisting of a concrete dowel in a 60 mm diameter hole in a greased perforated plate, were used to explore the shear capacity of concrete dowel within the hole. The bonded concrete dowel specimens, with bond at the plate/concrete interface and the same concrete dowel as that in the unbonded concrete dowel specimens, were used to investigate the combined action of interfacial bond and concrete dowel. The bonded rebar specimens, with a 20 mm diameter transverse rebar passed through a 21 mm diameter hole in the steel plate, were used to explore the combination of interfacial bond and the steel rebar dowel. In order to assess the capacity of the reinforced concrete dowel by hole, unbonded PBL specimens, with a 20 mm diameter steel rebar surrounded by a concrete dowel passing through a 60 mm diameter hole in the greased perforated plate, were tested. The standard PBL specimens, consisted of interfacial bond and the same reinforced concrete dowel as those for the unbonded PBL, were evaluated experimentally to examine the performance of the interface bond and reinforced concrete dowel.

By comparing the results of the above specimens, the influence of each parameter can be assessed. For example, the impact of steel fibers can be evaluated by specimens fabricated with RPC and RPCF; the effect of interface bond can be obtained by the bonded and unbonded specimens (*i.e. the bonded concrete dowel specimens and the unbonded concrete dowel specimens, the standard PBL specimens and the unbonded PBL specimens*); the influence of concrete dowel can be assessed through specimens with or without concrete dowels (*i.e. the bonded concrete dowel specimens and the pure bond specimens, the standard PBL specimens and the bonded rebar specimens*); and the influence of transverse rebar can be achieved through specimens with or without transverse rebar (*i.e. the bonded rebar specimens and the pure bond specimens, the unbonded concrete dowel specimens and the unbonded PBL specimens, the standard PBL specimens and the bonded concrete dowel specimens*).

All push-out specimens have the same outside dimensions, as shown in Fig. 2. The dimensions of the concrete blocks (*length* × *width* × *height*) are 400 mm × 400 mm × 450 mm. The overall dimensions of the perforated steel plates that are plugged into the concrete blocks are 300 mm × 555 mm × 25 mm (*width* × *height* × *thickness*). The embedment depth of the steel plate in concrete block is 400 mm. At the bottom end of the perforated steel plate, a 400 mm long, 25 mm wide, and 50 mm high empty slot is provided for the vertical displacement of the plate. For pure bond specimens (*i.e. groups R-b1r0d0 and RF-b1r0d0*), no holes were introduced to steel plate. However, for the bonded rebar specimens (*i.e. groups R-b1r1d0 and RF-b1r1d0*), a 21 mm diameter hole is drilled at the center of the steel plate. The perforated plate hole diameter for specimens in other groups is 60 mm. For specimens with transverse steel rebar, a 20 mm diameter steel rebar is provided at the center of the hole. Each concrete block is reinforced with 10 mm in diameter rectangular stirrups. The stirrups volumetric reinforcement ratio is 1.68%.

Table 1
Description of push-out test specimens.

Group	Specimen code	State	Components of resistance			Diameter of the hole D (mm)	Transverse rebar	
			Interfacial bond	Concrete dowel	Transverse rebar		Grade	Diameter d (mm)
1	R-b1r0d0	Pure bond	√			–	–	–
2	RF-b1r0d0							
3	R-b0r0d1	Unbonded concrete dowel		√		60	–	–
4	RF-b0r0d1							
5	R-b1r0d1	Bonded concrete dowel	√	√		60	–	–
6	RF-b1r0d1							
7	R-b1r1d0	Bonded rebar	√		√	21	HRB335	20
8	RF-b1r1d0						HRB400	
9	R-b0r1d1	Unbonded PBL		√	√	60	HRB335	20
10	RF-b0r1d1						HRB400	
11	R–b1r1d1	Standard PBL	√	√	√	60	HRB335	20
12	RF-b1r1d1						HRB400	

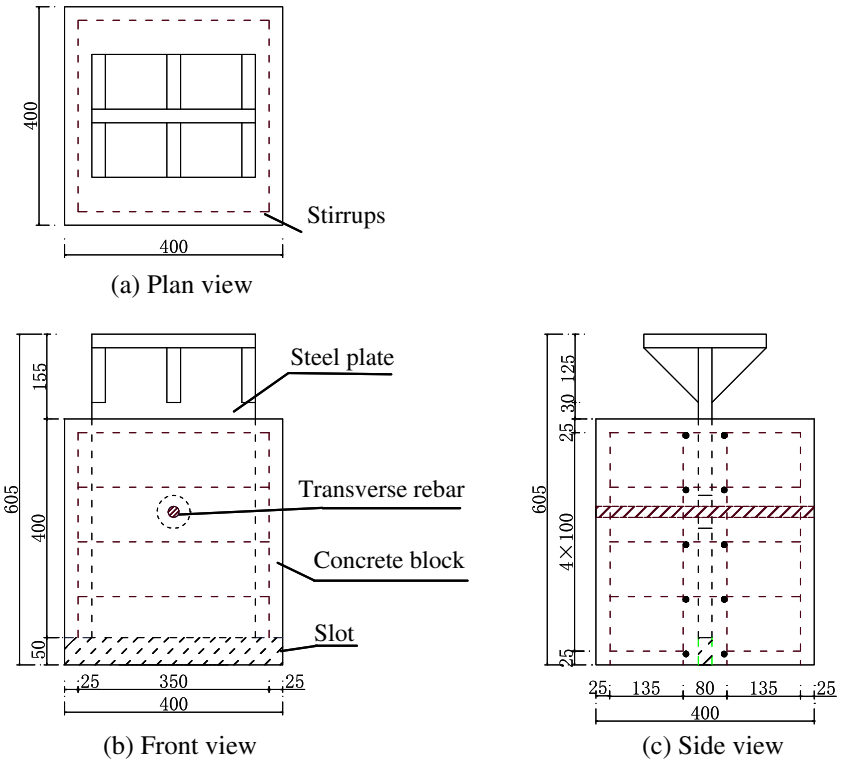

Fig. 2. Geometry of the tested specimens (R-b1r1d1 example, dimensions in mm).

2.2. Materials

The UHPC used in this study is a commercially available product of RPC. The RPC is composed of ordinary Portland cement, silica fume, quartz sand, ground quartz, water reducer and short steel fibers. Table 2 shows the mix proportions of the RPC. The average particle size of silica fume was 0.70 μm. The maximum particle size of quartz sand and ground quartz were 0.60 mm and 45.0 μm gradation, respectively. The steel fibers had a length of 15.0 mm, a diameter of 0.20 mm with a tensile strength of 2600 MPa. The RPC were cast using the concrete mix producing 100 MPa target compressive strength. Standard cubes with side length of 100 mm were used for determining the average compressive strength. In addition, 100 mm × 100 mm × 300 mm prisms were used for measuring the prismatic strength and average modulus of elasticity. Six specimens were tested and the average values are presented in Table 3, where the f_{cu} is the cubic compressive strength, f_{cp} is the prismatic strength, and E_c is the modulus of elasticity (Young's modulus)

The structural steel Q345C (*nominal yield stress of* 345 MPa) was used in all perforated steel plates. For groups R-b1r1d0, R-b0r1d1, and R-b1r1d1, steel rebars of HRB335 (*with a nominal yield stress of* 335 MPa) were positioned at the center of holes. For groups RF-b1r1d0, RF-b0r1d1, and RF-b1r1d1, HRB400 steel rebars (*nominal yield stress of* 400 MPa) were provided as transverse steel reinforcement. HPB235 steel stirrups with a nominal yield stress of 235 MPa were set in concrete blocks of all groups. Mechanical properties of steel rebars obtained from standard coupon tests are listed in Table 4, where the f_y is the yield strength, f_u is the ultimate tensile strength, E_s is the modulus of elasticity, and δ is the percentage elongation.

Table 3
Mechanical properties of the RPC.

Type	Average f_{cu} (MPa)	Average f_{cp} (MPa)	Average E_c (GPa)
RPC	115.5	92.6	42.6
RPCF	124.7	101.5	43.4

2.3. Fabrication of push-out test specimens

Wooden formworks were fabricated for casting all concrete blocks. Rectangular stirrups were prefabricated in the laboratory (Fig. 3a). On the bottom of perforated steel plate, a 400 mm long, 25 mm wide and 50 mm high polyethylene foam was attached prior to casting of concrete to provide a gap for the vertical slip of connector (*refer to* Fig. 3b). The perforated steel plates in the unbonded concrete dowel specimens (*i.e. groups R-b0r0d1 and RF-b0r0d1*) and the unbonded PBL specimens (*i.e. groups R-b0r1d1 and RF-b0r1d1*) were greased on the surfaces to eliminate any bond and friction effect between the plate and the concrete, whereas other specimens kept a naturally bonded interface. All specimens were air-cured in the laboratory for 28 days prior to testing (*see* Fig. 3c).

Table 2
RPC Mix design.

Relative weight ratios to cement							Steel fiber (V_f%)
Type	Cement	Silica fume	Quartz sand	Ground quartz	Water reducer	Water	
RPC	1.0	0.25	1.1	0.1	0.025	0.275	0%
RPCF							2%

Table 4
Mechanical properties of steel reinforcements.

Type	Steel grade	Diameter d (mm)	Average f_y (MPa)	Average f_u (MPa)	Average E_s (GPa)	δ (%)
Rebar in the concrete Block	HPB235	10	298	446	201	25
Transverse rebar in the PBL	HRB335	20	358	529	207	26
	HRB400		466	653	205	23

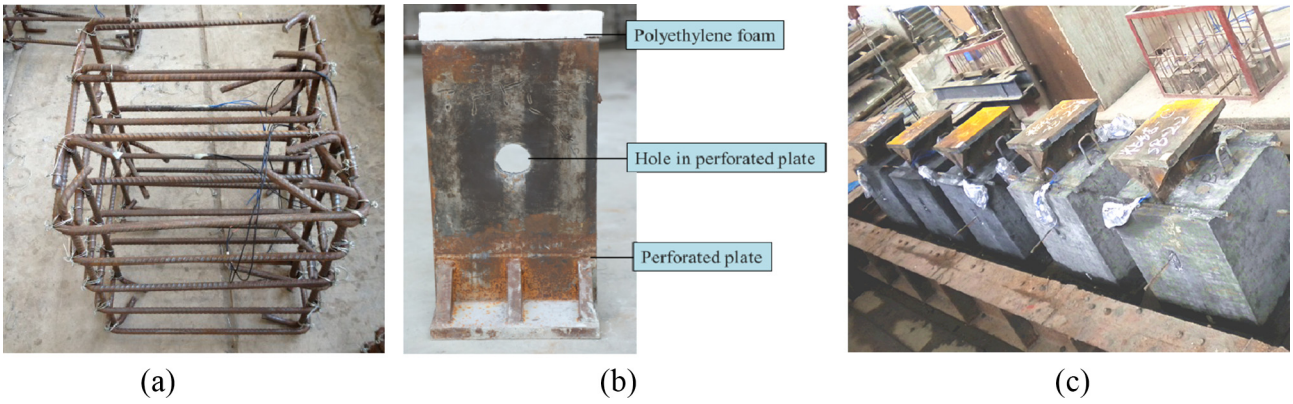

Fig. 3. Fabrication of push-out test specimens: (a) rectangular stirrups; (b) polyethylene foam at the end of steel plate; (c) curing of the push-out specimens.

2.4. Instrumentation and push-out test setup

The typical test setup used for all push-out tests is shown in Fig. 4. The vertical displacement of the steel plate was measured by two Linear Variable Differential Transformers (*LVDTs*) that were positioned at the opposite sides as shown in Fig. 4a. The LVDTs captured any steel plate/concrete slip, thus providing a measure of deformation of the dowel at the hole. The load was applied to the push-out specimens via a calibrated 2000 kN capacity Universal Testing Machine (*UTM*). Spherical hinge bearing that was positioned on the top of each push-out specimen was used to prevent any eccentricity of the applied compression load imposed on the steel perforated plate as shown in Fig. 4b.

The specimens were loaded in accordance with the procedure adapted by Candido-Martins et al. [19]. Once the initial applied load reached 10 kN, all LVDTs were reset to zero. The load was then applied in steps at an average rate of 5 kN per second up to the peak (ultimate) load, after which the steel plate load-controlled protocol was switched to a displacement-controlled protocol that was controlled at a rate of 0.2 mm per minute in order to captured the post-peak load curve. All automated measurements were recorded via a computerized data acquisition system.

3. Test results and discussion

3.1. Failure modes

The failure modes of push-out specimens involved the detachment of the steel plate and the fracture of the dowel. Perforated steel plates were removed from concrete blocks and no buckling was found in the steel plates of all specimens. For the RPCF specimens, no cracks were observed on the concrete blocks. This can be attributed to the use of the steel fibers in the concrete mix. For the RPC specimens, no cracks were detected on concrete blocks for

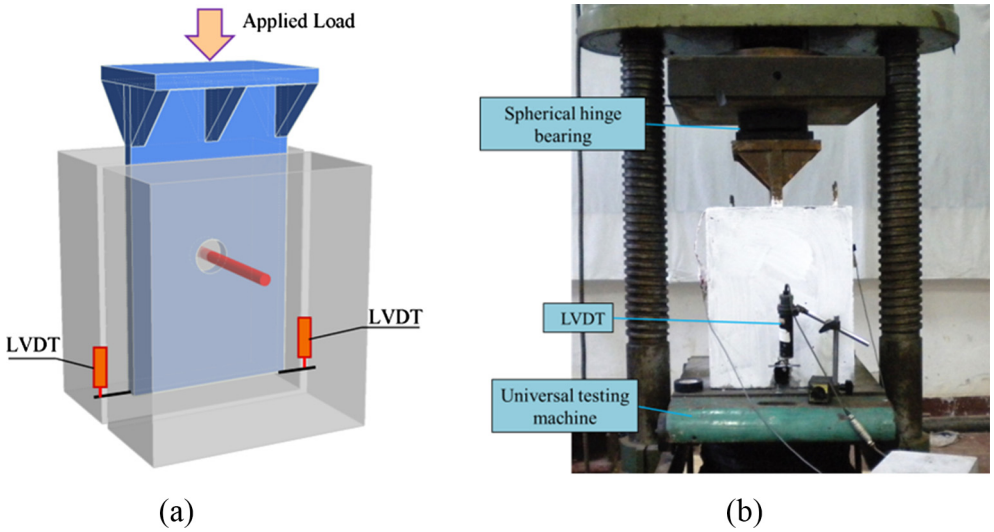

Fig. 4. Push-out test setup: (a) displacement measurement plan; (b) overall view of test setup.

specimens without transverse steel rebar in groups R-b1r0d0, R-b0r0d1 and R-b1r0d1. However, this was not the case for specimens of groups R-b1r1d0, R-b0r1d1 and R-b1r1d1 with transverse rebar where some cracks occurred with increasing applied load. A typical crack distribution on the side face of concrete blocks for R-b1r1d1 is presented in Fig. 5a.

By examining the failure mode of dowels through the hole after each test, it was found that failure occurred due to fracture of the dowels at the two side faces of the steel plate. Furthermore, the failure of the dowels barely varied by fibers content. For groups R-b0r0d1, R-b1r0d1, RF-b0r0d1, and RF-b1r0d1, only with concrete dowels, the concrete dowels sheared off directly at the steel plate/-concrete interfaces. For groups R-b1r1d0 and RF-b1r1d0, with a 20 mm diameter steel rebar at the 21 mm diameter hole and almost no concrete dowel surrounding the rebar, the transverse rebar was also sheared off directly at the plate/concrete interfaces. For groups R-b0r1d1, R-b1r1d1, RF-b0r1d1, and RF-b1r1d1, with a 20 mm diameter rebar inside concrete dowel passing through the 60 mm diameter hole, the transverse rebar presented a tension/shear failure mode, similar to PBL embedded in conventional concrete that were previously observed and reported by Wang et al. [6], Su et al. [8] and He et al. [22]. Fig. 5b plots the failure mode of the dowels inside the holes in perforated plates.

3.2. Load-slip curves

Fig. 6 shows the load-slip curves for all groups. The ultimate load (*peak load*), P_u, and the relative slip, S_u, at P_u are summarized in Table 5. As shown in the table, push-out specimens without transverse rebar produced a maximum average S_u of 1.67 mm; while specimens with a transverse rebar exhibited a much ductile behavior with a minimum average S_u of 7.52 mm that conformed with the required ductility in accordance with the Eurocode 4 [27]. Meanwhile, it is also noted that the ultimate loads achieved in RPCF groups were higher than those of the RPC groups. As can be calculated from the experimental data listed in Table 5, the ultimate loads of groups RF-b1r0d0, RF-b0r0d1, and RF-b1r0d1 were 1.82, 1.50 and 1.85 times those of groups R-b1r0d0, R-b0r0d1 and R-b1r0d1, respectively. The ultimate loads of groups RF-b1r1d0, RF-b0r1d1, and RF-b1r1d1 were 1.85, 1.12 and 1.42 times those of groups R-b1r1d0, R-b0r1d1, and R-b1r1d1, respectively.

The load-slip curves of the pure bond specimens (*i.e. groups R-b1r0d0 and RF-b1r0d0*) only with bond at the steel plate/concrete interface are plotted in Fig. 6a. One can see from this figure that adding 2% (*by volume*) steel fibers in UHPC, increased the ultimate load of RF-b1r0d0 by 82% as compared to that of R-b1r0d0. This can be ascribed to the steel fibers increased the shear strength of UHPC and restricted the growth of the crack propagation parallel to the plate near or along the plate/UHPC interface, and in addition to lead to large mechanical interlock and friction effects at the cracking surfaces [28]. No slip was observed at the bottom end of steel plates for groups R-b1r0d0 and RF-b1r0d0 up to 73–85% of their ultimate loads. However, for loads above this threshold (*and below ultimate load*), slip was developed slowly with increased applied load due to the gradual propagation of mechanical interlock and the generation of friction over the entire steel plate surface. Just after the ultimate load, slip increased rapidly and residual loads of 143 kN and 342 kN were identified from the curves produced for groups R-b1r0d0 and RF-b1r0d0, respectively. The average bond strength that was calculated by dividing the ultimate load by the total bonded interface area was 1.17 MPa for R-b1r0d0 and 2.13 MPa for RF-b1r0d0. The average residual bond strengths corresponding to the residual loads of groups R-b1r0d0 and RF-b1r0d0 were 0.48 MPa and 1.14 MPa, respectively.

The load-slip curves of the specimens with a concrete dowel inside a 60 mm diameter hole are presented in Fig. 6b and c. All applied loads to the unbonded concrete dowel specimens (*i.e. groups R-b0r0d1 and RF-b0r0d1*) were carried by the concrete dowel inside the hole. As shown in Fig. 6b, the slip increased linearly as the applied load increased up to the ultimate load. Due to the effect of fibers in increasing shear strength and deformability of concrete dowel, the ultimate load and associated relative slip of RF-b0r0d1 increased by 50% and 86%, respectively as compared to those of R-b0r0d1. As shown in Fig. 6c, the bonded concrete dowel specimens (*i.e. groups R-b1r0d1 and RF-b1r0d1*) consisted of interfacial bond and concrete dowel, no slips occurred up to a load level of approximately 75% of the peak loads. Following debonding of the specimens, the slip increased with increasing loads and failure was initiated as the load approached its peak. Similarly, and attributing to the improvement of the interfacial bond and shear capacity of concrete dowel, the ultimate load and relative slip of RF-b1r0d1 increased by 85% and 11%, respectively as compared to those of R-b1r0d1.

The load-slip curves of the bonded rebar specimens (*i.e. groups R-b1r1d0 and RF-b1r1d0*) with bond at plate/concrete interface and a 20 mm diameter transverse rebar inside the 21 mm diameter hole are presented in Fig. 6d. In this case, the steel plate and concrete were well bonded resulting virtually in no slip prior to plates debonding. After which, a linear increase of the slip was noticed with increasing load up to the end of elastic loading region that

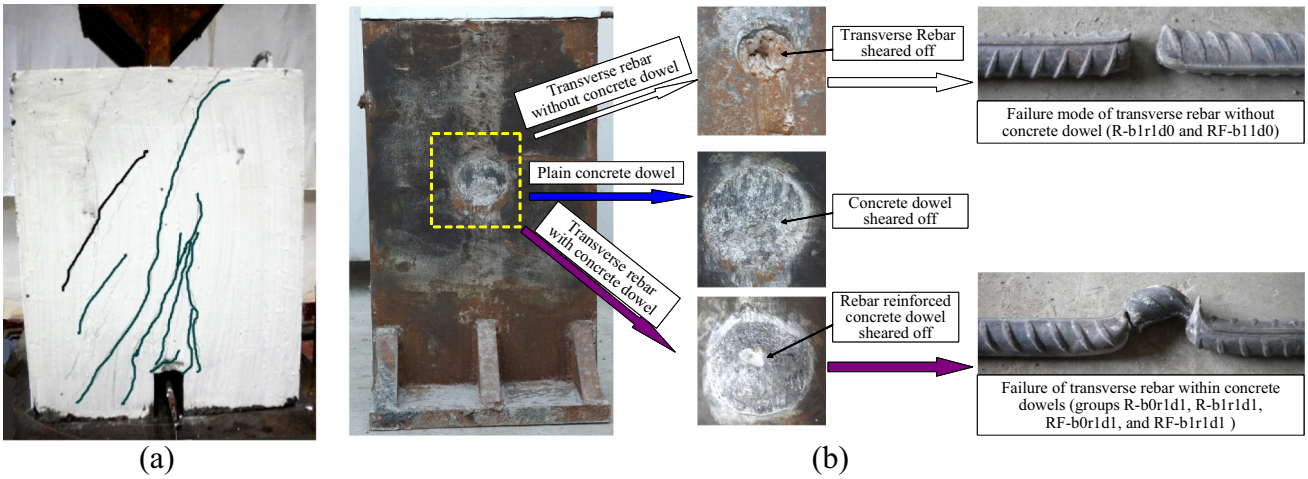

Fig. 5. Failure modes of tests: (a) crack pattern of concrete block; (b) failures of dowels within the holes.

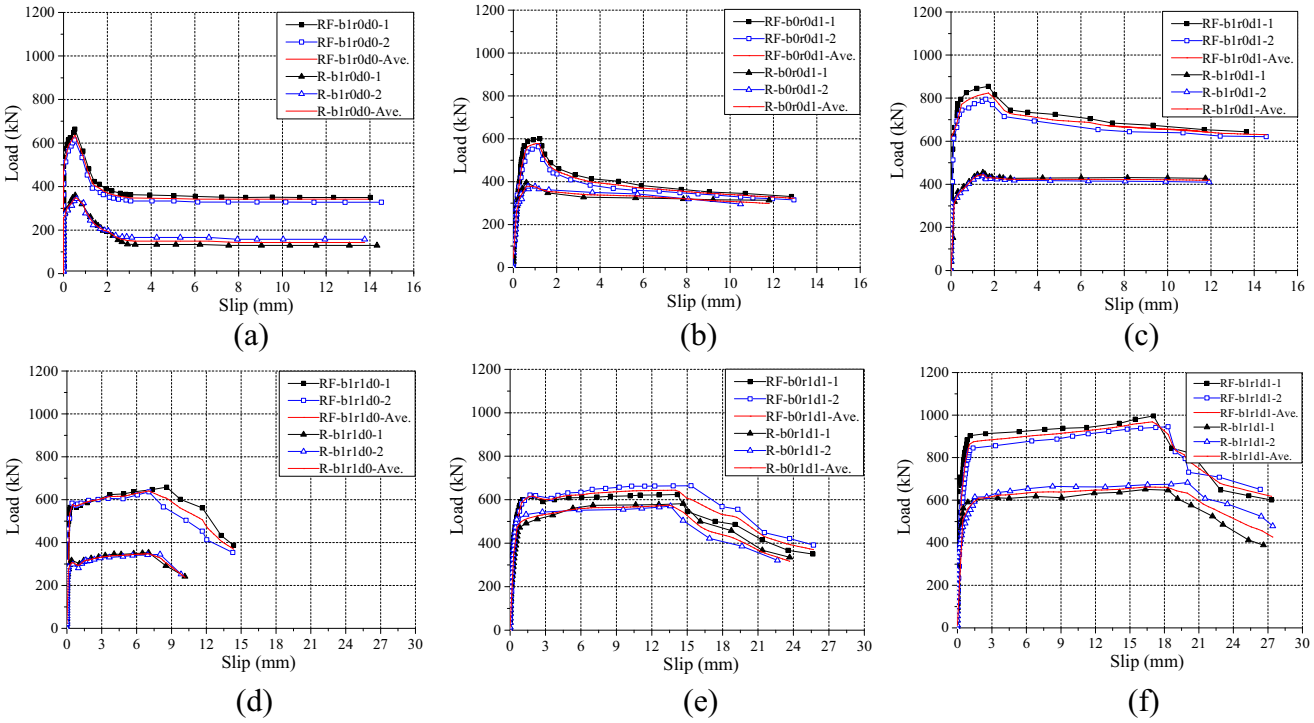

Fig. 6. Load-slip curves of push-out specimens: (a) pure bond specimens; (b) unbonded concrete dowel specimens; (c) bonded concrete dowel specimens; (d) bonded rebar specimens; (e) unbonded PBL specimens; and (f) standard PBL specimens.

Table 5
Push-out test summary results.

Specimen code	Ultimate load, P_u (kN)			Relative slip, S_u (mm)		
	Specimen-1	Specimen-2	Average	Specimen-1	Specimen-2	Average
R-b1r0d0	360	342	351	0.53	0.60	0.57
R-b0r0d1	396	378	387	0.60	0.68	0.64
R-b1r0d1	454	438	446	1.52	1.48	1.50
R-b1r1d0	353	345	349	7.01	8.02	7.52
R-b0r1d1	582	571	577	14.04	13.56	13.80
R-b1r1d1	651	683	667	16.34	20.02	18.18
RF-b1r0d0	664	614	639	0.55	0.51	0.53
RF-b0r0d1	601	563	582	1.22	1.16	1.19
RF-b1r0d1	855	795	825	1.73	1.61	1.67
RF-b1r1d0	658	636	647	8.58	7.06	7.82
RF-b0r1d1	624	665	645	14.17	15.44	14.31
RF-b1r1d1	982	905	944	17.11	18.32	17.67

corresponds to a load level of 308 kN for R-b1r1d0 and 574 kN for RF-b1r1d0. This can be translated to approximately 88% of their ultimate loads. Beyond this load level, the transverse rebar started to yield and the fracture after ultimate load was achieved. Attributing to the use of the fibers and the HRB400 grade steel rebar, the ultimate load and the relative slip of RF-b1r1d0 increased by 85% and 4%, respectively, as compared to those of R-b1r1d0 where transverse rebar was made of HRB335 steel grade.

The load-slip curves of the PBL specimens with a 20 mm diameter steel rebar inside concrete dowel in a 60 mm diameter hole are plotted in Fig. 6e and f. As shown in Fig. 6e, the unbonded PBL specimens (*i.e. groups R-b0r1d1 and RF-b0r1d1*) exhibited linear behaviors starting from the initial slip to the reinforced dowel yielding that corresponds to a load equal to 503 kN for R-b0r1d1 and 601 kN for RF-b0r1d1. These loads are approximately 90% of their ultimate loads. Beyond this load level, stiffness degradation was observed while linear behavior was maintained up to the ultimate loads. As compared to R-b0r1d1, the use of steel fibers and HRB400 transverse reinforcement resulted in increasing both the ultimate load and the relative slip of RF-b0r1d1 by 12% and 4%, respectively. On the other hand, and as shown in Fig. 6f, the load-slip curves for the standard PBL (*i.e. groups R-b1r1d1 and RF-b1r1d1*) were similar to other bonded specimens where no slip was observed prior to debonding. As the load increased, slip was linearly proportional to loads approximately equal to 90% of their ultimate loads. The sudden drop in curves of groups R-b1r1d1 and RF-b1r1d1 indicated the fracture of the rebar dowel by hole. The presence of steel fibers and the use of HRB400 transverse reinforcement contributed in increasing the shear capacity of interfacial bond and transverse rebar. In this case, the ultimate load of specimen RF-b1r1d1 increased by 42% as compared to specimen R-b1r1d1 with HRB335 steel grade rebar. The similar deformability of HRB400 and HRB335 rebars resulted in a similar relative slip of groups R-b1r1d1 and RF-b1r1d1, with a slip equal to 18.18 mm for R-b1r1d1 and 17.67 mm for RF-b1r1d1. Apparently, the bond resistance at the plate/concrete interface, the action of concrete dowel

in shear, and the overall resistant-capacity of a PBL connector were effectively improved by the adding steel fibers to the concrete mix. However, the slip capacity of the connectors seems to be barely improved by adding fibers except for the unbonded concrete dowel specimens (*i.e. groups R-b0r0d1 and RF-b0r0d1*), with a slip capacity increase of 86%.

3.3. Effects of interfacial bond between perforated plate and concrete

Effects of bond at the plate/concrete interface were investigated using the bonded specimens (*i.e. groups R-b1r0d1, R-b1r1d1, RF-b1r0d1, and RF-b1r1d1*) and the unbonded counter-part specimens (*i.e. groups R-b0r0d1, R-b0r1d1, RF-b0r0d1, and RF-b0r1d1*). As shown in Table 5, improvements in both ultimate load and relative slip were identified for the bonded specimens as compared to the unbonded specimens. For example, the ultimate load and relative slip of specimen R-b1r0d1 increased by 15% and 134%, respectively as compared to specimen R-b0r0d1. The corresponding improvements for specimen R-b1r1d1 were 16% and 32%, respectively as compared to specimen R-b0r1d1. Results presented in Table 5 indicate that the ultimate load and relative slip of specimen RF-b1r0d1 increased by 42% and 40%, respectively as compared to specimen RF-b0r0d1; whereas 46% in ultimate load and 23% in relative slip increase were observed for specimen RF-b1r1d1 as compared to specimen RF-b0r1d1. Generally and as compared to the unbonded specimens, the ultimate loads of all bonded specimens with RPC and RPCF have increased by approximately 15% and 42%, respectively, with relative slip improvements that ranged from 23% to 134%.

In order to further investigate the effect of the interfacial bond, the contribution of bond to the overall resistant-capacity of those bonded specimens was isolated by comparing the average load-slip curves for the different specimens evaluated in this study in accordance with the compatibility of slip deformation. Here, assume that the contribution of interface bond to the overall shear-resistant capacity in those bonded specimens other than the pure bond ones is equal to that in the pure bond specimens at the same slip. This is acceptable because all bonded specimens from different groups in present tests have the same bonded area, material properties and contacting state at the steel plate/concrete interface. Fig. 7a shows the average load-slip curves from groups RF-b1r0d1 and RF-b1r0d0. The difference between groups RF-b1r0d1 and RF-b1r0d0 is the former group has a concrete dowel by the hole while the latter does not have. As shown in Fig. 7a, the average ultimate load and relative slip (S_u) of RF-b1r0d1 were 825 kN and 1.67 mm, respectively. According to the slip deformation compatibility between the specimens in groups RF-b1r0d1 and RF-b1r0d0, at the S_u of 1.67 mm of RF-b1r0d1, the shear-resistant capacity of bond on the steel plate interface should be approximately equal to 400 kN, which was the residual load capacity of interface bond in specimen RF-b1r0d0 at the slip of 1.67 mm. As such, the contribution of the interfacial bond on overall resistant-capacity of RF-b1r0d1 is achieved. Using the same methodology, one can calculate the contributions of interfacial bond for groups R-b1r0d1, R-b1r1d1 and RF-b1r1d1. These results are presented in Fig. 7b.

As shown in Fig. 7b, a range of 43–48% of the ultimate resistances of the bonded concrete dowel specimens are provided through interfacial bond. Comparatively, the contribution of interfacial bond in the overall resistance of standard PBL with RPC and RPCF are 21% and 36%, respectively. The contribution of bond in a standard PBL, with conventional concrete was determined by the results of the authors' previous research [22] to be 26%. The interfacial bond in PBL at ultimate state is mainly provided by residual friction at the plate/concrete interface. The average friction strength between steel plate and conventional concrete is 0.51 MPa [22], while those for steel plates embedded in RPC and RPCF obtained from present tests are 0.48 MPa and 1.14 MPa, respectively. The higher friction strength led to a stronger friction resistance at the contact surface, which resulted in a higher contribution proportion to the bond in the PBL detail. It should be noted that the contribution of interfacial bond to the structural performance of PBL, in superimposed beams, is considered to be relatively small and usually is ignored in design [17]. However, the preceding results indicate that ignoring the contribution of interface bond to the PBL in steel-concrete joint would lead to a much conservative design. As such, the contribution of interfacial bond should be accounted for in the design of PBL in steel-concrete joint of hybrid bridge girders.

3.4. Effects of concrete dowel

The effect of concrete dowels was evaluated by comparing experimental results obtained from specimens with concrete dowels (*i.e. groups R-b1r0d1, R-b1r1d1, RF-b1r0d1, and RF-b1r1d1*) and those without concrete dowels (*i.e. groups R-b1r0d0, R-b1r1d0, RF-b1r0d0, and RF-b1r1d0*). Table 5 shows that the ultimate load and relative slip of RPC specimens with a concrete dowel inserted

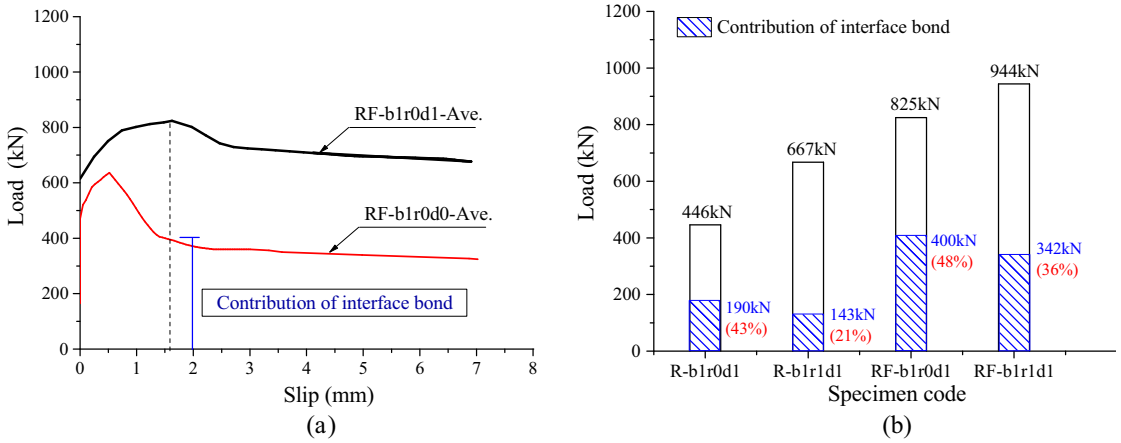

Fig. 7. Individual contribution of interfacial bond: (a) decomposition of the contribution by interface bond in overall resistance of RF-b1r0d1; (b) proportions of interfacial bond in overall resistant of push-out specimens (proportion = interfacial bond effect/ultimate load).

through a 60 mm diameter hole (*such as R-b1r0d1*) have increased by 27% and 160%, respectively as compared to R-b1r0d0. Also, the corresponding improvements of both ultimate load and relative slip for specimen R-b1r1d1 are 91% and 140%, respectively as compared to specimen R-b1r1d0. For RPCF specimens, a comparison between RF-b1r0d1 and RF-b1r0d0 indicates that providing a concrete dowel inside the hole resulted in an increase in both the ultimate load capacity and the relative slip by 29% and 220%, respectively; whereas the increases in ultimate load and relative slip between RF-b1r1d1 and RF-b1r1d0 were 46% and 130%, respectively. These results confirm the achievement of remarkable improvements in both ultimate load and relative slip of the connectors when concrete dowels are utilized. This performance enhancement can be attributed to the fact that the bearing capacity of transverse rebar, under tension/shear failure mode in groups R-b1r1d1 and RF-b1r1d1, was higher than that of the steel rebar that was sheared off for groups R-b1r1d0 and RF-b1r1d0 (*refer to* Fig. 5b).

Similar to the discussion of bonding effects, the contributions of the concrete dowel to the overall resistant-capacity of the connectors were isolated using the load-slip curves. Assume that the contribution of concrete dowel to the overall shear-resistant capacity in those specimens with a concrete dowel is equal to that in the unbonded concrete dowel specimens at the same slip, which is acceptable since all specimens with a concrete dowel in present tests have the same material properties and geometric dimensions for the concrete dowels. Fig. 8a shows the average load-slip curves from groups RF-b1r0d1 and RF-b0r0d1. As can be seen, according to the slip deformation compatibility between the specimens in groups RF-b1r0d1 and RF-b0r0d1, at the S_u of 1.67 mm of RF-b1r0d1, the shear-resistant capacity of the concrete dowel in RF-b1r0d1 should be approximately equal to 420 kN, which was the shear-resistant capacity of concrete dowel in specimen RF-b0r0d1 at the slip of 1.67 mm. Using this methodology, the contribution of concrete dowel in groups R-b1r0d1, R-b0r1d1, R-b1r1d1, RF-b0r1d1, and RF-b1r1d1 are obtained and summarized in Fig. 8b.

As shown in Fig. 8b, about 51–69% of the overall resistances of the bonded concrete dowel specimens and the unbonded PBL specimens are provided by the concrete dowel. The contribution of the concrete dowel to the overall resistance of standard PBL with RPC and RPCF are 41% and 34%, respectively, whereas the contribution of concrete dowel in a standard PBL, with conventional concrete was determined by the results of the authors' previous research [22] to be 28%. It should be emphasized that the only difference between the PBL with conventional concrete [22] and PBL with RPC evaluated in this study is the concrete compressive strength. Based on the experimental results, the individual resistance provided by concrete dowel in a standard PBL with RPC and RPCF were 274 kN and 323 kN, respectively, while for PBL with conventional concrete [22], the individual resistance was 154 kN. It is apparent that the shear resistance of the concrete dowel was improved proportionally with the increase in concrete compressive strength. Moreover, a comparison between the experimental results of R-b1r1d1 and RF-b1r1d1 indicates that the individual resistance of concrete dowel was also increased by adding fibers to the concrete mix up to 18%.

3.5. Effects of transverse steel rebar

The effect of using a transverse steel rebar was assessed using the experimental results of specimens with transverse rebar (*i.e. groups R-b1r1d0, R-b0r1d1, R-b1r1d1, RF-b1r1d0, RF-b0r1d1, and RF-b1r1d1*) and those specimens without transverse rebar (*i.e. groups R-b1r0d0, R-b0r0d1, R-b1r0d1, RF-b1r0d0, RF-b0r0d1,and RF-b1r0d1*). As shown in Table 5, for the bonded rebar specimens (*i.e. groups R-b1r1d0 and RF-b1r1d0*) with a 20 mm diameter transverse steel rebar inside a 21 mm diameter hole, the relative slip of groups R-b1r1d0 and RF-b1r1d0 increased by approximately 13 times as compared to those obtained from groups R-b1r0d0 and RF-b1r0d0 without the steel rebars. In contrast, the ultimate loads of groups R-b1r1d0 and RF-b1r1d0 only increased by 1% when compared to those of groups R-b1r0d0 and RF-b1r0d0. The hardly increased ultimate loads demonstrated that the combined actions of residual interfacial friction and 20 mm diameter steel rebar dowel in groups R-b1r1d0 and RF-b1r1d0 approximately equal to the peak interfacial bonding strength of groups R-b1r0d0 and RF-b1r0d0. Providing a transverse rebar inside the concrete dowel for specimen R-b0r1d1 increased both ultimate load and relative slip by 49% and 21 times, respectively as compared to the R-b0r0d1 specimen; For R-b1r1d1 specimen, the corresponding improvements were 50% and 11 times, respectively as compared to the ultimate load capacity and the relative slip of specimen R-b1r0d1. A comparison between experimental results obtained from groups RF-b0r1d1 and RF-b0r0d1 indicates that the use of a transverse steel rebar inside the concrete dowel increased both the ultimate load capacity and the relative slip by 11% and 11 times, respectively; whereas the corresponding improvements for specimen RF-b1r1d1 were 14% and 10 times, respectively as compared to specimen RF-b1r0d1. Based on the experimental results, it is clear that the relative slip of specimens with a transverse steel

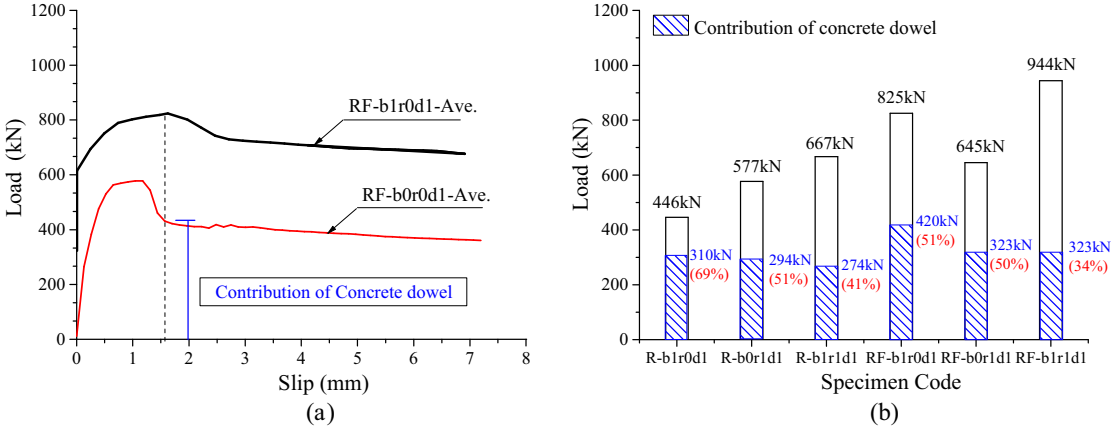

Fig. 8. Individual contribution of concrete dowel: (a) decomposition of the contribution by concrete dowel in overall resistance of RF-b1r0d1; (b) proportions of concrete dowel in overall resistant of push-out specimens (proportion = effect of concrete dowel in shear/ultimate load).

rebar were 10 to 21 times higher than those without transverse steel rebar detail. This indicates that the bulk of slip capacity of the connectors is provided by the transverse steel rebar.

In order to investigate the individual contribution of the transverse steel rebar, load differences between the load-slip curves of groups R-b0r1d1, R-b1r1d1, RF-b0r1d1, and RF-b1r1d1 with transverse rebar reinforced concrete dowels and groups with pure concrete dowels (*i.e. groups R-b0r0d1, R-b1r0d1, RF-b0r0d1, RF-b1r0d1*) are isolated. According to the compatibility of slip deformation, the contribution of transverse rebar should approximately equal to the associate load difference. Fig. 9a presents the average load-slip curves from groups RF-b1r1d1 and RF-b1r0d1. As shown in Fig. 9a, according to the compatibility of the slip deformation between specimens RF-b1r1d1 and RF-b1r0d1, at the S_u of 17.67 mm of RF-b1r1d1, the shear-resistant capacity of transverse steel rebar in RF-b1r1d1 should be approximately equal to 311 kN, which was the load difference between the load-slip curves of RF-b1r1d1 and RF-b1r0d1 at the slip of 17.67 mm. Using this methodology, the contribution of transverse steel rebar in groups R-b0r1d1, R-b1r1d1, RF-b0r1d1 are obtained and summarized in Fig. 9b.

Fig. 9b shows that 45–48% of the overall resistances of the unbonded PBL specimens are supplied by transverse rebars. The proportions of transverse rebars in the overall resistances of R-b1r1d1 and RF-b1r1d1 are about 35% and 33%, respectively, while for PBL specimen with conventional concrete is 44% [22]. For the HRB335 transverse steel rebar installed in the PBL specimen using conventional concrete and RPC, it was found that the individual resistance by the steel rebar are 256 kN [22] and 237 kN, respectively. The relatively small difference between the two individual resistance values can be attributed to the variation of the HRB335 steel rebar strength used from two different batches. For the HRB400 transverse steel rebar that was used in RF-b1r1d1, the individual resistance of the rebar is 311 kN which is about 1.30 times the 237 kN steel rebar resistance that was used in specimen R-b1r1d1. Referring to the reinforcement properties presented in Table 4, the strength of HRB400 rebar in RPCF specimens was about 1.30 times that of the HRB335 rebar used in RPC specimens. Therefore, one can be concluded that the shear capacity of transverse steel rebar in PBL specimen increases linearly with the rebar strength, which in return, indicates that the individual resistance of transverse rebar in PBL was barely influenced by concrete types and presence of fibers in the mix.

4. Proposed shear resistance formulas for PBL connectors

4.1. Existing PBL shear capacity equations

Currently, several equations were proposed to predict the ultimate resistance of PBL connectors based on push-out experimental results performed on PBL in steel-concrete superimposed beams with conventional concrete slabs. However, few equations exist to determine the ultimate resistance of PBL connectors with UHPC in steel-concrete joint of hybrid girders. Some typical equations for the resistance prediction of PBL connectors are listed in Table 6

In order to assess the applicability of the existing equations to PBL with UHPC in steel-concrete joint of hybrid girder, the preceding equations are implemented beyond their applicable range. The ultimate resistance of PBL was computed for the unbonded PBL and the standard PBL connectors. The ratios between the predicted ultimate strength to the experimentally obtained ultimate resistance were calculated in order to evaluate the results. Table 7 presents a summary of ratios between the predicted by different equations presented earlier and the experimental results.

From Table 7, one can see that the shear capacity for the connectors was overestimated by Eqs. (1)–(4), with an average $V_u^{Pre.}/V_u^{Exp.}$ ratio ranging from 1.30 to 6.21. Eq. (1) was proposed based on experimental results obtained from push-out tests for PBL with conventional concrete in superposed beams. In these tests, PBLs failed due to the yield of steel components between the adjacent holes, which was significantly different from the dowel fracture failure mode observed in the present work. Also, the shear capacity of PBL with UHPC was seriously overestimated by Eqs. (2) and (3). For example, the ratio between prediction value obtained from Eq. (2) and actual test results reached up to 7.12 for R-b0r1d1. This major difference between the analytical and experimental values can be attributed to the fact that predicted resistances produced by Eqs. (2) and (3) included the effect of local bearing concrete at the bottom end of the perforated plate, while the experimental results in present work did not contain the effect because the local bearing concrete was removed before conducting the test. Eq. (4) was developed for the connector with normal concrete and without interface bond, and the suggested correction coefficient for the concrete shear strength suggested was to be 5, which may be not applicable for the PBL with UHPC in present work. In contrast, Eqs. (5)–(7) gave comparatively safe results, with average $V_u^{Pre.}/V_u^{Exp.}$ ratios ranging from 0.85 to 0.87. Both Eqs. (5) and (6) resulted in a better correlation with the experimental

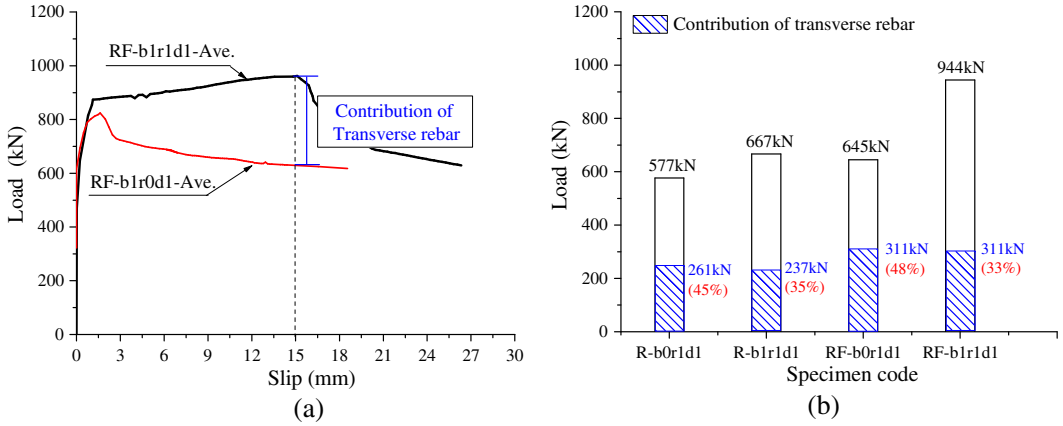

Fig. 9. Individual contribution of transverse rebar: (a) decomposition of the contribution by transverse rebar in overall resistance of RF-b1r1d1; (b) proportions of transverse rebar in overall resistant of push-out specimens (proportion = effect of transverse rebar /ultimate load).

Table 6
Some typical models for the shear resistance of PBL.

Authors	Predicting models	Notation
Leonhardt [5] Eq. (1)	$V_u = 2.553D^2 f'_c$	V_u: Shear capacity of connector (kN) D: Diameter of the hole (mm) f'_c: Cylinder concrete strength (MPa) q_u: Shear capacity of connector (kN) h: Height of connector (mm) t: Thickness of connector (mm) n: Number of the hole d: Diameter of the hole (mm) A_{tr}: Area of transverse rebar in concrete (mm^2) f_{yr}: Yield strength of reinforcement (MPa) f_{ck}: Cylinder concrete strength (MPa) h_{sc}: Height of connector (mm) t_{sc}: Thickness of connector (mm) A_{sc}: Area of end bearing concrete (mm^2) f_y: Yield tensile strength of reinforcement (MPa) A_s: Area of transverse rebar by the hole (mm^2) A_c: Area of concrete dowel by the hole (mm^2) Q_u: Nominal shear capacity of connector (kN) τ_{cu}: Nominal shear strength of concrete (MPa) τ_{sy}: Yield shear strength of rebar (MPa) α_c: Correction coefficient for shear strength k: Coefficient for direct shear test of short beam f_{cu}: Cubic compressive strength (MPa) f_t: Tensile strength of concrete (MPa) β: Correction factor τ_{su}: Ultimate shear strength of rebar (MPa) α_A: Effective shear area ratio of concrete dowel A: Area of the hole (mm^2) f_c: Cylinder concrete strength (MPa) d_s: Diameter of the rebar by the hole (mm) τ_b: Bond strength at plate/concrete interface (MPa) A_b: Area of plate/concrete bonded interface (mm^2)
Oguejiofor et al. [12] Eq. (2)	$q_u = 4.50htf'_c + 3.31nd^2\sqrt{f'_c} + 0.91A_{tr}f_{yr}$	
Vianna et al. [20] Eq. (3)	For $f_{ck} \leqslant 30$ MPa $q_u = 152.9 + 3.21 \times 10^{-3}(h_{sc}t_{sc}f_{ck}) - 0.86 \times 10^{-3}A_{sc}\sqrt{f_{ck}}$ For $f_{ck} > 30$ MPa $q_u = 31.8 + 1.9 \times 10^{-3}(h_{sc}t_{sc}f_{ck}) + 0.53 \times 10^{-3}(A_{tr}f_y) - 0.6 \times 10^{-6}(A_{sc}\sqrt{f_{ck}})$	
Su et al. [9] Eq. (4)	For $A_s(\beta A_s\tau_{su} - \tau_{sy}) \leqslant A_c\tau_{cu}$ $Q_u = A_c\tau_{cu} + A_s\tau_{sy}$ $\tau_{cu} = \alpha_c k\sqrt{f_{cu}f_t}$ For $A_s(\beta A_s\tau_{su} - \tau_{sy}) > A_c\tau_{cu}$ $Q_u = \beta A_s\tau_{su}$	
Zheng et al. [21] Eq. (5)	$V_u = 1.76\alpha_A(A - A_s)f_c + 1.58A_sf_y$ $\alpha_A = 3.80(A_s/A)^{2/3}$	
JSCE [29] Eq. (6)	$V_u = 1.45[(D^2 - d_s^2)f'_c + d_s^2f_y] - 106.1 \times 10^3$ $73.2 \times 10^3 < (D^2 - d_s^2)f'_c + d_s^2f_y < 488 \times 10^3$	
He et al. [22] Eq. (7)	$V_u = \tau_bA_b + 1.06\frac{\pi(D^2-d_s^2)}{4}f_{cu} + 2.09\frac{\pi d_s^2}{4}f_y$ $\tau_b = -0.022f_{cu} + 0.306\sqrt{f_{cu}} - 0.573$	

Table 7
Comparison of equations to predict ultimate PBL resistance.

Specimen code	$V_u^{Pre.}/V_u^{Exp.}$							
	Leonhardt [5] Eq. (1)	Oguejiofor [12] Eq. (2)	Vianna [20] Eq. (3)	Su [9] Eq. (4)	Zheng [21] Eq. (5)	JSCE [29] Eq. (6)	He [22] Eq. (7)	Proposed Eq. (18)
R-b0r1d1	1.53	7.12	3.04	1.30	0.95	0.95	0.94	0.94
R-b1r1d1	1.32	6.16	2.63	–	0.82	0.82	0.89	1.01
RF-b0r1d1	1.48	6.87	2.92	1.30	0.96	0.97	0.96	1.01
RF-b1r1d1	1.01	4.69	2.00	–	0.65	0.66	0.69	0.97
Average	1.34	6.21	2.65	1.30	0.85	0.85	0.87	0.98

Note: $V_u^{Pre.}$ = *ultimate shear resistance determined from relative equations;* $V_u^{Exp.}$ = *experimental obtained ultimate load of a shear connector.*

results for the unbonded PBL (*i.e. groups R-b0r1d1 and RF-b0r1d1*) as compared to the standard PBL (*i.e. groups R-b1r1d1 and RF-b1r1d1*). This can be ascribed to the fact that these two equations were developed based on test data conducted on PBL connectors using conventional concrete with comparatively lower strength and the contact area between the steel plate and the concrete, in their push-out tests, was smaller than that in those adopted in current study tests. Eq. (7) showed better accuracy in predicting the ultimate resistance of all specimens except for specimen RF-b1r1d1. The conservative results obtained for RF-b1r1d1 was due to the fact that the bond strength between plate and UHPC computed by the expression of τ_b in Eq. (7) was only 0.17 MPa for RPC and 0.27 MPa for RPCF, that are much smaller than the 0.48 MPa for RPC and 1.14 MPa for RPCF obtained from tests conducted in the present study.

4.2. Proposed shear capacity equation and verification

As described earlier, the majority of the proposed equations overestimate the capacity of PBL connectors. The shear capacity of PBL connectors with conventional concrete obtained from the equations described earlier did not correlate well with the experimental results obtained from PBL with UHPC in this present study. In order to evaluate the ultimate resistance of PBL with UHPC in steel-concrete joint of hybrid girders, test results and the Eq. (7) are used as a basis for modification in order to account for the influence of the fibers and the high strength UHPC on the shear capacity of the members in PBL.

The rationale behind the Eq. (7) is to account for a cumulative contribution of the shear transfer through the interface bond V_{bv} (kN), the concrete dowel action V_{cv} (kN) and the transverse rebar action V_{sv} (kN), respectively.

$$V_u = V_{bv} + V_{cv} + V_{sv} \tag{8}$$

The individual contributions of V_{bv}, V_{cv} and V_{sv} to the overall shear resistance of PBL in current test were obtained from Sections 3.3–3.5, as summarized in Table 8. The estimated resistance exhibits close agreement with the experimental results, which indicates that the shear resistance of a PBL with UHPC could also be computed by adding the contributions of the interface bond, the concrete and the transverse rebar dowels on the basis of the compatibility of the slip deformation at the ultimate load.

Table 8
Components of PBL Shear Resistance.

Specimen Code	Measured Shear resistance (kN)	Contribution of Each Part (kN)			Estimated Shear Resistance (kN)	Estimated Measured
		Interfacial Bond	Concrete dowel	Transverse rebar		
R-b1r1d1	667	143	274	237	654	0.98
RF-b1r1d1	944	342	323	311	976	1.03

As indicted above, the interfacial bond between steel plate and UHPC cannot be evaluated well by expression for bond strength between steel plate and conventional concrete in the Eq. (7). For this reason, a more applicable approach for predicting the interfacial bond, τ_b, are needed to account for V_{bv} with UHPC. According to recent literature review, there is no published data on predicting the bond strength for flat steel plate embedded in UHPC. The approach for the bond strength between steel rebar and plain UHPC without any fibers described in the literature [30] concluded that the bond strength was related to the square-root of the concrete strength. Accordingly, the expression for the bond between flat steel plate and plain UHPC without any fibers is defined as:

$$\tau_b = \alpha\sqrt{f_{cu}} \tag{9}$$

For bond strength between flat plate and fiber reinforced UHPC, and according to the theory of composite materials, the bond strength can be modified by introducing a fiber factor K_f [28,31],

$$\tau_{bf} = K_f \times \tau_b \tag{10}$$

where τ_{bf} = the residual bond stress between flat plate and fiber reinforced UHPC (MPa).

The factor K_f given in [31] is expressed as

$$K_f = 1 + \beta\left(V_f\frac{L_f}{\phi_f}\right) \tag{11}$$

where β = coefficient to be determined by experiment; V_f = volume content of fibers; L_f = average length of fibers (mm); ϕ_f = normalized diameter of fibers (mm).

Due to the lack of test data for residual bond strength between flat steel plate and UHPC in the literature, the value of coefficients in Eqs. (9)–(11) is obtained based on the current experimental results. In present work, the values of L_f and ϕ_f are 15 mm and 0.2 mm, respectively. Experimental results show that the $\tau_{bf} = 0.48$ MPa when $f_{cu} = 115.5$ MPa, $V_f = 0\%$, and the $\tau_{bf} = 1.14$ MPa when $f_{cu} = 124.7$ MPa, $V_f = 2\%$. Therefore, the value of $\alpha = 0.04$ and $\beta = 1.03$ can be obtained. The bond strength between flat plate and UHPC in PBL connector can be calculated by:

$$\tau_{bf} = 0.04\left(1 + 1.03\frac{V_f L_f}{\phi_f}\right)\sqrt{f_{cu}} = \left(0.04 + 0.04\frac{V_f L_f}{\phi_f}\right)\sqrt{f_{cu}} \tag{12}$$

Therefore, the contribution of interface bond can be calculated by:

$$V_b = \tau_{bf} \times A_b = \left(0.04 + 0.04V_f\frac{L_f}{\phi_f}\right)A_b\sqrt{f_{cu}} \tag{13}$$

CECS Code [32] gives the following formula to determine the shear capacity of the fiber reinforced concrete.

$$V_{cv} = \left(1 + \gamma V_f\frac{L_f}{\phi_f}\right)V_c \tag{14}$$

where γ = coefficient to be determined; V_c = shear resistance provided by concrete without fibers (kN).

As discussed earlier, the shear capacity of concrete dowel increases with increasing concrete compressive strength. Therefore, the following expression for conventional concrete dowel in the Eq. (7) is used to account for V_c:

$$V_c = 1.06\frac{\pi(D^2 - d_s^2)}{4}f_{cu} \tag{15}$$

A value of $\gamma = 0.07$ can be obtained on the basis of the current test results using Eqs. (14) and (15). Now, the resistance of the concrete dowel in the hole can be calculated by:

$$V_{cv} = 1.06\left(1 + 0.07V_f\frac{L_f}{\phi_f}\right)\frac{\pi(D^2 - d_s^2)}{4}f_{cu} = \left(1.06 + 0.07V_f\frac{L_f}{\phi_f}\right)\frac{\pi(D^2 - d_s^2)}{4}f_{cu} \tag{16}$$

In terms of the contribution of transverse steel rebar, test observations and discussion on effects of using transverse steel rebar indicated that the shear capacity of transverse rebar in PBL linearly increases with increasing rebar strength and the individual contribution of transverse rebar was barely influenced by concrete types and fibers. Based on these facts, the resistance provided by transverse rebar can be calculated by the rebar contribution term in the Eq. (7) and is expressed by the following equation:

$$V_{sv} = 2.09\frac{\pi d_s^2 f_y}{4} \tag{17}$$

Hence, the ultimate shear capacity of a standard PBL connector with UHPC in steel-concrete joint of hybrid girder can be calculated by the following relation:

$$V_u = \left(0.04 + 0.04V_f\frac{L_f}{\phi_f}\right)A_b\sqrt{f_{cu}} + \left(1.06 + 0.07V_f\frac{L_f}{\phi_f}\right)\frac{\pi(D^2 - d_s^2)}{4}f_{cu} + 2.09\frac{\pi d_s^2}{4}f_y \tag{18}$$

The ultimate resistance estimations for PBL with UHPC obtained from Eq. (18) are presented in Table 7. The predicted results show a good agreement with those obtained from tests for PBL using

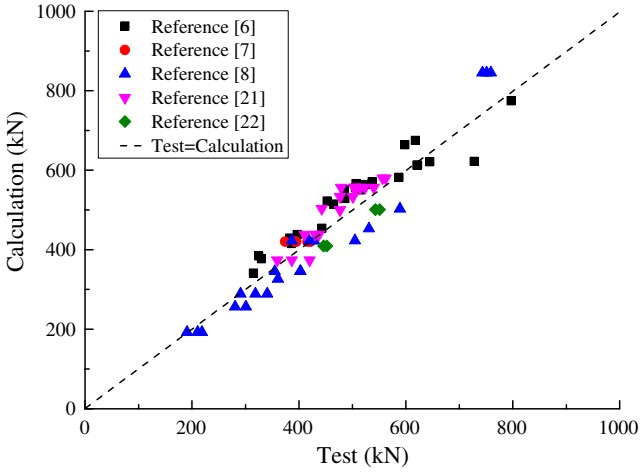

Fig. 10. Comparison between tests and calculations.

UHPC, with an average ratio of 0.98. Additionally, as Eq. (18) was modified from Eq. (7) which was developed for the evaluation of PBL with conventional concrete in steel-concrete joints, the related experimental results obtained by the third parties Wang et al. [6], He et al. [7], Su et al. [8], Zheng [21], and authors' previous research [22] were introduced to assess the applicability of Eq. (18) to PBL using conventional concrete in steel-concrete joint in hybrid girders. Fig. 10 shows the comparison of the experimental and predicted results. The mean value and the standard deviation are 1.05 and 0.04, respectively; the coefficient of determination and the Pearson Coefficient are 0.90 and 0.95, respectively, which demonstrates that the Eq. (18) can be potentially used to predict the ultimate resistance of PBL in steel-concrete joint of hybrid girders with both UHPC and conventional concrete. However, the authors suggest that more push-out test data of the PBL with UHPC in hybrid girders are needed to verify the applicability of the proposed empirical equations.

5. Conclusions

This paper focuses on examining the shear transfer behavior of PBL with UHPC designed for the connectors in steel-concrete joint of hybrid girders. Twenty-four push-out tests were performed to investigate the effects of interface bond, concrete dowel and transverse rebar in the hole on PBL. The load transferring mechanism and equations to predict the ultimate resistance of the PBL in steel-concrete joint of hybrid girders are discussed. The main conclusions from the study are as follows:

1. The high performance of the UHPC result in preventing brittle cracking failure of concrete blocks surrounding PBL. With the use of 2% vol. steel fibers and HRB400 grade rebars, the ultimate resistance of PBL embedded in fiber reinforced UHPC are 1.12 to 1.42 times those obtained from the counter-parts using plain UHPC without any fibers.
2. The average bond strength for a flat steel plate with plain UHPC and fiber reinforced UHPC are 1.17 MPa and 2.13 MPa, respectively. The ultimate resistance of the connectors with interfacial bond using fiber reinforced UHPC is approximately 1.15 times those of the unboned count-parts, and ultimate resistance obtained from the bonded connectors using plain UHPC is about 1.42 times those of the unbonded count-parts.
3. Providing a concrete dowel surrounding transverse rebar increases the ultimate resistance of a standard PBL using fiber reinforced UHPC and plain UHPC by 46% and 91%, respectively as compared to specimens without concrete dowels, and the individual contribution of concrete dowel in PBL is improved by adding fibers to the concrete mix.
4. The bulk of slip capacity of PBLs is determined by the action of transverse rebar by the hole. The shear capacity of transverse rebar in PBL is linearly increased with the rebar strength and the individual resistance of transverse rebar is barely influenced by concrete types and fibers.
5. The proportions of the interface bond, the concrete dowel in shear and the transverse rebar action in a standard PBL with plain UHPC are approximately 21%, 41% and 35%, respectively; whereas the proportions for a standard PBL embedded in fibrous UHPC are around 36%, 34% and 33%, respectively.
6. The ultimate resistance of PBL predicted by the empirical equation compares relatively well with that obtained experimentally. Although the proposed equation can be potentially used to evaluate the ultimate resistance of the PBL with UHPC, the authors suggest that more push-out test data and analysis are needed to verify its applicability.

Acknowledgements

This research is sponsored by the National Natural Science Foundation of China (Grant No. 51278182), and the program of China Scholarship Council (File No. 201506130024). These supports are gratefully acknowledged. The support of the Civil & Environmental Engineering Department at the University of California, Irvine, USA is also gratefully acknowledged.

Reference

[1] Su Q, Yang G, Bradford MA. Static behaviour of multi-row stud shear connectors in high-strength concrete. Steel Compos Struct 2014;17(6):967–80.
[2] Su Q, Yang G, Bradford MA. Bearing capacity of stud-bolt hybrid shear connection in segmental composite bridge girders. J Bridge Eng 2016;21(4):06015008.
[3] Liu X, Bradford MA, Lee MSS. Behavior of high-strength friction-grip bolted shear connectors in sustainable composite beams. J Struct Eng 2015;141(6):04014149.
[4] Ali SNH, Ramli S, Meldi S, Mahdi S. Various types of shear connectors in composite structures: a review. Int J Phys Sci 2012;7(22):2876–90.
[5] Leonhard F, Andra W, Andra HP, Harre W. New, Improved bonding means for composite load bearing structures with high fatigue strength. Beton Stahlbetonbau 1987;82(12):325–31.
[6] Wang W, Zhao C, Li Q, Zhuang W. Study on load-slip characteristic curves of perfobond shear connectors in hybrid structures. J Adv Concr Technol 2014;12:413–24.
[7] He J, Liu Y, Pei B. Experimental study of the steel-concrete connection in hybrid cable-stayed bridges. J Perform Constr Facil 2014;28(3):559–70.
[8] Su Q, Wang W, Luan H, Yang G. Experimental research on bearing mechanism of perfobond rib shear connectors. J Constr Steel Res 2014;95:22–31.
[9] Su Q, Yang G, Bradford MA. Bearing capacity of perfobond rib shear connectors in composite girder bridges. J Bridge Eng 2016;21(4):06015009.
[10] Peter H. Economical shear connectors with high fatigue strength. In: International association for bridge and structural engineering, Iabse symposium Brussels; 1990. p. 167–72.
[11] Oguejiofor EC, Hosain MU. Parametric study of perfobond rib shear connectors. Can J Civ Eng 1993;21:614–25.
[12] Oguejiofor EC, Hosain MU. Numerical analysis of push-out specimens with perfobond rib connectors. Comput Struct 1997;62(4):617–24.
[13] Ahn JH, Lee CG, Won JH, Kim SH. Shear resistance of the perfobond-rib shear connector depending on concrete strength and rib arrangement. J Constr Steel Res 2010;66(10):1295–307.
[14] Studnicka J, Machacek J, Krpata A. Perforated shear connector for composite steel and concrete beams. In: Composite construction in steel and concrete, Banff, Alberta, Canada; 2002. p. 367–78.
[15] Valente I, Cruz PJS. Experimental analysis of perfobond shear connection between steel and lightweight concrete. J Constr Steel Res 2004;60(3):465–79.
[16] Valente I, Cruz PJS. Experimental analysis of shear connection between steel and lightweight concrete. J Constr Steel Res 2009;65(10):1954–63.
[17] Medberry SB, Shahrooz BM. Perfobond shear connectors for composite construction. Eng J 2002;39(1):2–12.
[18] Al-Darzi SYK, Chen A, Liu Y. Finite element simulation and parametric studies of perfobond rib connector. Am J Appl Sci 2007;4(3):122–7.
[19] Candido-Martins JPS, Costa-Neves LF, Vellasco PCGS. Experimental evaluation of the structural response of perfobond shear connectors. Eng Struct 2010;32(8):1976–85.
[20] Vianna JC, Andrade SAL, Vellasco PCGS, Costa-Neves LF. Experimental study of Perfobond shear connectors in composite construction. J Constr Steel Res 2013;81:62–75.
[21] Zheng S, Liu Y, Yoda T, Lin W. Parametric study on shear capacity of circular-hole and long-hole perfobond shear connector. J Constr Steel Res 2016;117:64–80.
[22] He S, Fang Z, Fang Y, Liu M, Liu L, Mosallam A. Experimental study on perfobond strip connector in steel-concrete joints of hybrid bridges. J Constr Steel Res 2016;118:169–79.
[23] Hegger J, Feldmann M, Rauscher S, Hechler O. High-performance materials in composite construction. Struct Eng Int 2009;4:438–46.
[24] Hegger J, Gallwoszus J, Rauscher S. Load-carrying behavior of connectors under shear, tension and compression in ultra high performance concrete. RWTH Aachen University, Institute of Structural Concrete, Aachen; 2009.
[25] Kang JY, Park JS, Jung WT, Keum MS. Evaluation of the shear strength of perfobond rib connectors in ultra high performance concrete. Engineering 2014;6:989–99.
[26] Wirojjanapirom P, Matsumoto K, Kono K, Kitamura T, Niwa J. Experimental study on shear behavior of PBL joint connections for UFC-PC hybrid girder. J JSCE 2014;2:285–98.
[27] EUROCODE 4. EN 1994-1-1. Design of composite steel and concrete structures Part 1. 1 General rules and rules for buildings. Brussels: CEN-European Committee for Standardization; 2005.
[28] Huang L, Chi Y, Xu L, Chen P, Zhang A. Local bond performance of rebar embedded in steel-polypropylene hybrid fiber reinforced concrete under monotonic and cyclic loading. Constr Build Mater 2016;103:77–92.

[29] Standard specifications for steel and composite structures. Japan Society of Civil Engineers (JSCE); Dec. 2009.
[30] Yoo DY, Shin H, Yang JM, Yoon YS. Material and bond properties of ultra-high performance fiber reinforced concrete with micro steel fibers. Compos B 2014;58:122–33.
[31] Harajli MH, Hamad B, Karam K. Bond-slip response of reinforcing bars embedded in plain and fiber concrete. J Mater Civ Eng 2002;14:503–11.
[32] CECS 38:92. Specification for design and construction of steel fiber reinforced concrete structures. Beijing: China Association for Engineering Construction Standardization; 1992 (In Chinese).